Inactivation of Calcium Channel Current in the Calf Cardiac Purkinje Fiber

Evidence for Voltage- and Calcium-mediated Mechanisms

ROBERT S. KASS and MICHAEL C. SANGUINETTI

From the Department of Physiology, School of Medicine and Dentistry, University of Rochester, Rochester, New York 14642

ABSTRACT We have studied the influence of divalent cations on Ca channel current in the calf cardiac Purkinje fiber to determine whether this current inactivates by voltage- or Ca-mediated mechanisms, or by a combination of the two. We measured the reversal (or zero current) potential of the current when Ba, Sr, or Ca were the permeant divalent cations and determined that depletion of charge carrier does not account for time-dependent relaxation of Ca channel current in these preparations. Inactivation of Ca channel current persists when Ba or Sr replaces Ca as the permeant divalent cation, but the voltage dependence of the rate of inactivation is markedly changed. This effect cannot be explained by changes in external surface charge. Instead, we interpret the results as evidence that inactivation is both voltage and Ca dependent. Inactivation of Sr or Ba currents reflects a voltage-dependent process. When Ca is the divalent charge carrier, an additional effect is observed: the rate of inactivation is increased as Ca enters during depolarizing pulses, perhaps because of an additional Ca-dependent mechanism.

INTRODUCTION

As reviewed recently by Tsien (1983) and Hagiwara and Byerly (1981), it now appears that several types of Ca channels exist. One criterion for comparison is the manner in which current through the channels decays with time or inactivates. Some Ca channels show little or no inactivation, but those that do inactivate appear to do so by a voltage-dependent process, by an intracellular Ca-mediated process, or by a combined mechanism (for review, see Eckert et al., 1981).

Two observations crucial to the Ca_i-mediated inactivation hypothesis are (*a*) decay of Ca channel current is slowed or absent when Ba or Sr replaces extracellular Ca (Ca_o), and (*b*) inactivation produced by a prepulse varies with Ca entry during that prepulse (Eckert et al., 1981). Observations that favor voltage-

Address reprint requests to Dr. Robert S. Kass, Dept. of Physiology, Box 642, School of Medicine and Dentistry, University of Rochester, 601 Elmwood Ave., Rochester, NY 14642.

J. GEN. PHYSIOL. © The Rockefeller University Press · 0022-1295/84/11/705/22$1.00 705
Volume 84 November 1984 705–726

dependent inactivation in other cells are the findings that (*a*) the rate of inactivation in these cells increases monotonically with depolarization (and can be significant at potentials too weak to activate Ca entry), and (*b*) the time course of inactivation is not significantly changed by replacing Ca_o with Ba or Sr (Fox, 1981).

Initial reports of Ca channel current in multicellular cardiac preparations interpreted the decay of this current as a voltage-dependent process (for review, see Reuter, 1979; Coraboeuf, 1980). More recently, several studies in multicellular and single-cell cardiac preparations have presented evidence that this process is a Ca_i-mediated phenomenon (Marban and Tsien, 1981; H. F. Brown et al., 1981; Fischmeister, 1981; Hume and Giles, 1982).

The purpose of this study was to determine systematically whether Ca channel current in the cardiac Purkinje fiber inactivates by a voltage-dependent process, a Ca-dependent process, or by a combination of the two mechanisms. These experiments provide the first quantitative description of the kinetics of Ca channel current inactivation in the calf cardiac Purkinje fiber after outward currents have been blocked. Our results show that inactivation of this current persists when Ba or Sr replaces Ca_o, and that this inactivation satisfies the criteria for a voltage-dependent process. When Ca^{2+} is the permeant divalent cation, the decay of this current is characterized by both a voltage-mediated and another (presumably Ca-mediated) mechanism.

METHODS

Calf hearts were obtained at a local slaughterhouse and transported to the laboratory in cold (4°C) Tyrode solution continuously gassed with 100% O_2. The transport time from removal of the heart from the animal to arrival in the laboratory averaged 15 min. Purkinje fiber cell bundles (100–200 μm diam) were removed from either ventricle, shortened (0.5–1.5 mm), and placed in warmed (35°C) oxygenated Tyrode solution until used.

Measurement of Membrane Current

Membrane current was measured with a conventional two-microelectrode voltage-clamp technique (Siegelbaum and Tsien, 1980) with electrode spacings appropriate for the measurement of inward current (Kass et al., 1979). This procedure allows accurate resolution of the time course of inactivation of Ca^{2+} channel current, but it is not fast enough to measure the rapid transient tail currents caused by deactivation of the channels (Kass et al., 1979). Current signals were filtered at 1 kHz, digitized, and recorded by a PDP 1123 computer (Digital Equipment Corp., Maynard, MA). Ca channel current was measured during depolarizing voltage steps applied from appropriate holding potentials. Because Ca is not the only permeant divalent charge carrier used in this study, we refer to current through this channel as Ca channel current.

Microelectrodes were pulled from thin-walled omega-dot glass (Glass Co. of America, Bargaintown, NJ) and then beveled using a modified spin-bar beveler. Voltage-measuring microelectrodes were filled with 3 M KCl. Current-passing electrodes were filled with 1.5 M tetrabutylammonium (TBA) Cl (Sigma Chemical Co., St. Louis, MO), or with 1.5 M K-citrate.

Solutions and Drugs

The standard Tyrode solution contained 150 mM NaCl, 4 mM KCl, 5.4 mM $CaCl_2$, 0.5 mM $MgCl_2$, 5 mM glucose, and 10 mM Tris (pH 7.4). Appropriate concentrations of $SrCl_2$ or $BaCl_2$ were used as $CaCl_2$ replacements, and the total divalent cation concentration was kept at 5.9 mM. All solutions were gassed with 100% O_2.

In experiments in which $CaCl_2$ was replaced by either $SrCl_2$ or $BaCl_2$, we found it necessary to allow at least 20 min for the preparation to equilibrate in the new solution before Ca channel currents reached a steady state. We found that Purkinje fibers were able to tolerate Ca-free, Sr-containing solutions, but after 30–40 min in Ca-free, Ba-containing solutions, the holding current became largely inward, cells uncoupled, and impalements became difficult to maintain. Similar effects of $BaCl_2$ on calf Purkinje fibers have been noted by Siegelbaum and Tsien (1980). Deterioration of the preparations after prolonged exposure to Ba-containing solutions restricted the number of experiments with Ba currents we could carry out in the absence and presence of a Ca channel blocking agent.

Iontophoretic injection of TBA was carried out to block the two time-dependent outward currents that contribute to Purkinje fiber plateau current: the delayed rectifier (I_x) and the transient outward current (I_{to}) (Kass et al., 1982). This injection procedure generally results in an ~90% blockade of delayed rectifier channels. In experiments in which further ionic substitution or drug subtraction procedures are not followed, this residual component of outward current can distort our measurements of Ca^{2+} channel current kinetics. Na current was eliminated by choice of holding potential or by addition of tetrodotoxin (TTX, 10 μM) (Calbiochem-Behring Corp., La Jolla, CA).

Ca channel current was blocked by exposing preparations to nisoldipine (10 μM) while voltage pulses were applied from a depolarized holding potential. In any given experiment, the pulse frequency and holding potential were constant before and after addition of the drug. Under these conditions, Ca channel currents are completely blocked and the block is not modulated by membrane potential (Kass, 1982). We chose to use nisoldipine as it has minimal effects on I_x (Kass, 1982). Thus, any possible contribution to measured current made by residual I_x that may not have been blocked by TBA will be minimized by analyzing drug-dissected records. Nisoldipine was dissolved in polyethylene glycol 400 to make a stock concentration of 10 mM. Aliquots of this stock solution were added directly to the Tyrode solution to obtain final concentrations. Nisoldipine experiments were carried out under subdued laboratory illumination as previously described (Kass, 1982). Nisoldipine was kindly supplied by Miles Laboratories, Inc., New Haven, CT.

Curve-fitting Procedures

Theoretical curves were fit to experimental data using a gradient expansion algorithm (Marquardt, 1963) that has been described by Bevington (1969). This procedure provides a method for determining a least-squares fit to an arbitrary function. Using the algorithms described by Bevington, we fit a general function of two (or one) exponential terms plus a baseline to our data:

$$y(t) = A_1 e^{-t/\tau_1} + A_2 e^{-t/\tau_2} + A_3.$$

The same technique was used to determine the time courses of inactivation during a voltage step and of recovery from an inactivating prepulse. In the analysis of all our experiments in which the time course of inactivation during a test pulse was examined (with sufficiently long test pulses), inactivation was best described as a function with two exponential components as determined by the χ^2 for either least-squares fit.

We used the same procedure to fit functions to our steady state activation and inactivation data by simply changing the general fitted function in the program.

RESULTS

Measurement of Ca Channel Current in the Purkinje Fiber

EXPERIMENTAL CRITERIA To reliably study mechanisms of Ca channel current inactivation, it was first necessary to demonstrate that time-dependent changes in membrane current during depolarizing voltage steps were due to Ca channel current and not to other current components or to depletion of charge carrier.

In this work, we blocked overlapping outward currents by iontophoretic injection of TBA (see Methods) before all experiments designed to investigate Ca channel current. We also found that replacement of Ca_o by Ba blocked I_{to} (as had been reported by Siegelbaum and Tsien, 1980) and I_x. Evidence for the reduction of both of these currents by Ba substitution is presented in Fig. 1. Thus, in the experiments described below for Ba-containing solutions, I_{to} and I_x are blocked both by intracellular TBA and the ionic composition of the superfusate.

CA CHANNEL CURRENT REVERSAL POTENTIAL As mentioned above, measurement of Ca channel current required block of I_x and I_{to} by TBA injection. The adequacy of this block was assessed by measuring currents near the Ca channel reversal (or zero current) potential following an approach similar to that

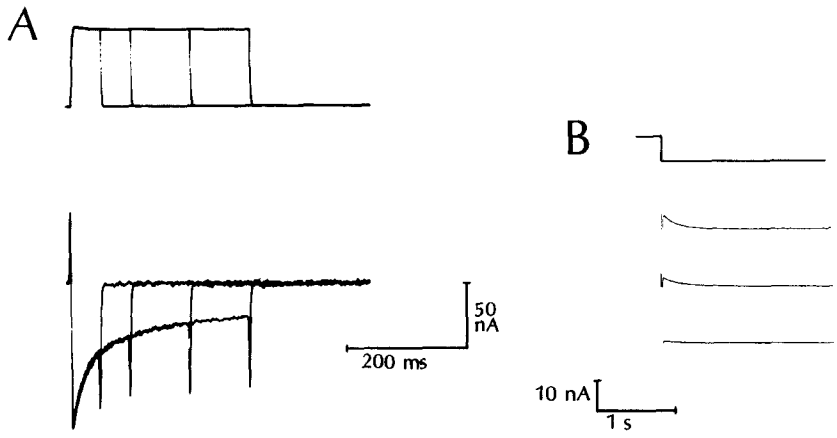

FIGURE 1. Replacement of extracellular Ca by Ba blocks I_{to} and I_x in the absence of intracellular TBA. (*A*) I_{to} tails (Fozzard and Hiraoka, 1973; Marban and Tsien, 1982) are abolished in Ba-containing Tyrode solution. Membrane current is shown in response to voltage pulses from −50 to +2 mV. Pulse durations are 50, 100, 200, and 300 ms. No I_{to} tail currents accompany the break of these pulses. 5.4 mM Ba Tyrode. Preparation 311-3. (*B*) Outward (I_x) current tails recorded before (upper trace) and 5 (middle) and 15 min (lower trace) after replacing Ca_o by 2.7 mM Ba. The tails were recorded after 250-ms voltage steps to −3 mV from a −30-mV holding potential, applied at 0.2 Hz. Preparation 311-1.

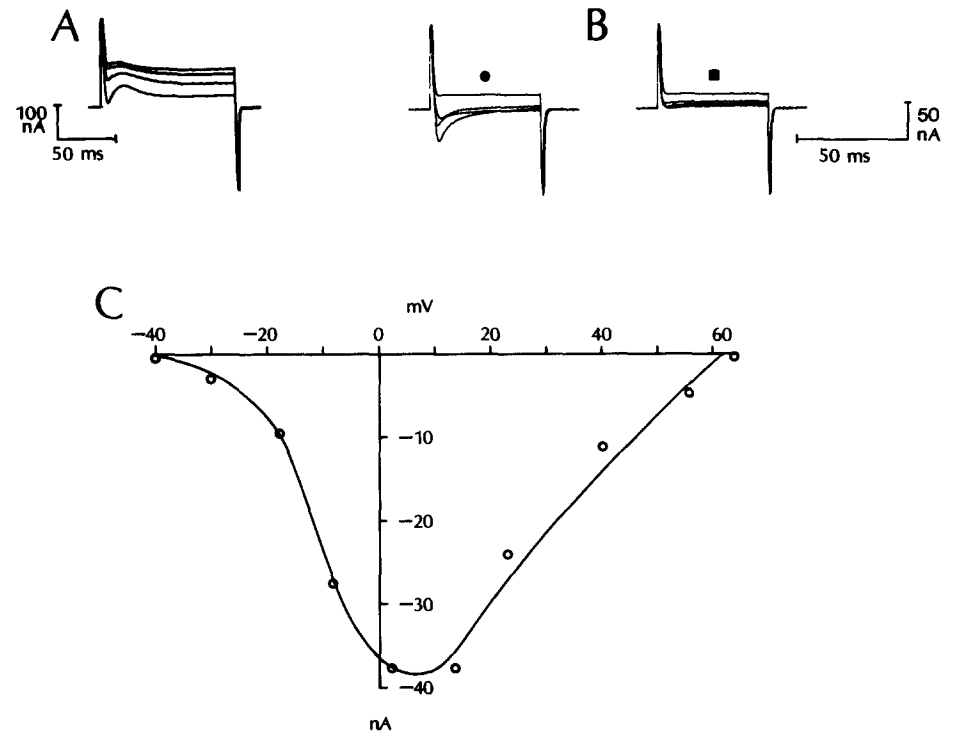

FIGURE 2. Ca channel reversal potential in Ca-containing solutions. (*A*) The transient outward current masks the Ca current reversal potential in a fiber that had not been injected with TBA. Currents are shown in response to voltage pulses to +10, +30, +55, and +68 mV from a −52-mV holding potential. Preparation 309-2. (*B*) Measurement of Ca current after TBA injection. Current traces are shown in response to pulses to −18, +2, +23, and +63 mV after blocking outward currents by injecting TBA. Background currents measured in the presence of nisoldipine (10 μM, ■) were subtracted from drug-free records (●) to obtain the Ca channel current. (*C*) Peak inward Ca channel current is plotted against pulse voltage. Holding potential (HP), −63 mV. Preparation 292-2.

applied to Ca channel current in single dialyzed heart cells (Lee and Tsien, 1982). At this potential, current through the channel will vanish and reveal any other time-dependent current. Furthermore, time-dependent current that does reverse at this potential should be blocked by a known Ca channel blocker. The results of our experiments are shown in Figs. 2 and 3.

Fig. 2 shows the results of experiments in Ca-containing solutions, and indicates the importance of TBA injection. Panel *A* shows current traces obtained in a fiber that had not been injected with TBA, and it is clear that the transient outward current obscures any reversal of Ca channel current that may be occurring in this voltage range. Panel *B* shows that after TBA injection, the time-dependent inward current vanishes as the membrane potential approaches +63 mV, and this time-dependent current is blocked by the Ca channel blocker nisoldipine (10 μM). As was the case for single dialyzed heart cells (Lee and

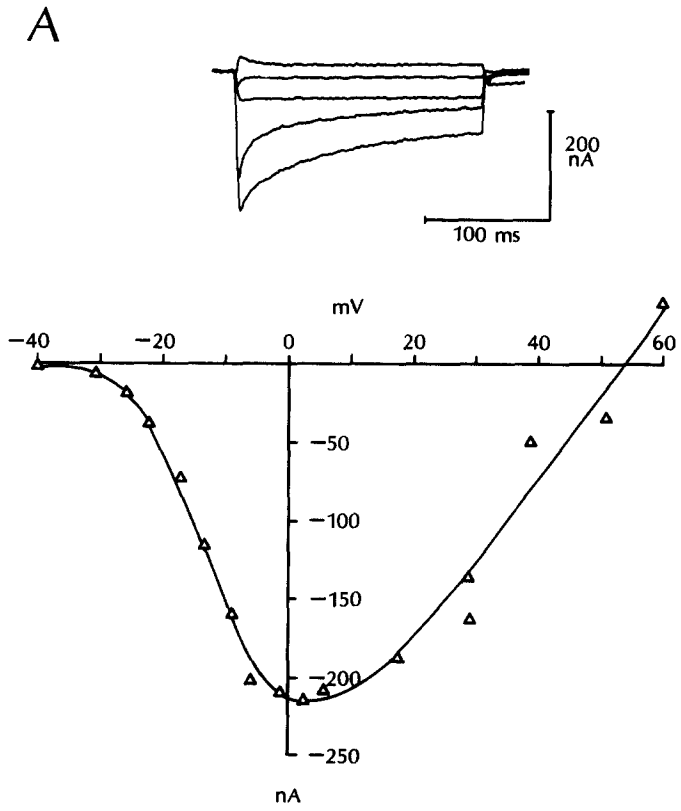

FIGURE 3. Ca channel current measured in Sr- and Ba-containing solutions: reversal potential measurements. Each panel shows Ca channel current records obtained by subtraction of background currents (measured in the presence of 10 μM nisoldipine) and the current-voltage relation peak inward (or maximum outward) current. (*A*) Current traces are shown in response to voltage pulses to (bottom trace to top trace) +2, +19, −22, +50, and +60 mV. V_{rev} is near +53 mV. 5.4 mM Sr Tyrode solution; HP, −50 mV. Preparation 301-3. (*B*) Current traces are shown in response to pulses to (bottom to top trace) −8, −22, +35, and +64 mV. V_{rev} is near +52 mV. 5.4 mM Ba Tyrode solution; HP, −40 mV. Preparation 322-2.

Tsien, 1982), membrane current at this potential is not affected by the drug, which indicates that the background current is not altered by this blocker.

The background current, measured in the presence of nisoldipine, contained leakage as well as capacity currents. This background current was subtracted from the drug-free records to determine the current-voltage relation for Ca channel current. When Ca is the divalent cation charge carrier, inward current reaches a maximum near +10 mV and approaches zero for depolarizations near +60 mV (*C*).

We found it very difficult to measure outward current through the Ca channel with Ca^{2+} as the charge carrier, but, as shown in Fig. 3, a clear reversal of this current can be observed when Ba^{2+} (or Sr^{2+}) is the permeant divalent cation.

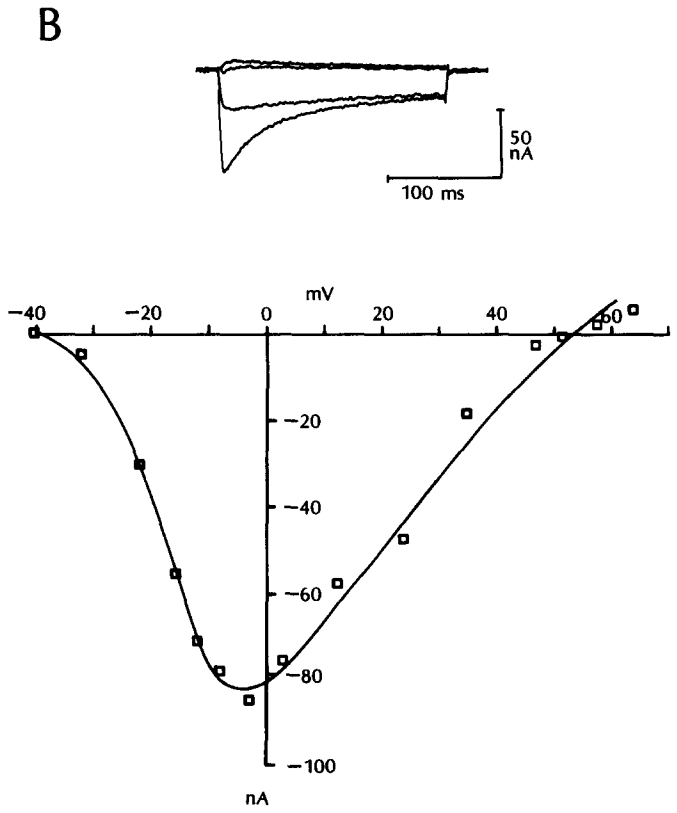

FIGURE 3*B*.

The insets in Fig. 3 show current records after background currents (measured in the presence of nisoldipine) had been subtracted. When Ca^{2+} was replaced by either of these ions, larger peak inward currents were recorded and maxima of the current-voltage curves were near 0 mV (Fig. 3).

The Ca channel reversal potential measured under the conditions of our experiments was 59 ± 5.7 mV (n = 3) with Ca^{2+} outside (measured as a zero-current potential), 48 ± 1.7 mV (n = 9) with Sr^{2+} outside, and 50 mV (n = 2) with Ba^{2+} outside.

TESTS FOR DEPLETION OF CHARGE CARRIER The reversal potential experiments confirm that I_x and I_{to} do not contribute time dependence to membrane current under the conditions of these experiments. Nevertheless, because the calf Purkinje fiber is a multicellular preparation, it is possible that depletion of charge carrier from a restricted extracellular space might contribute to the time dependence of measured inward currents (Bers, 1983; Hilgemann et al., 1983; Dresdner et al., 1982; Attwell et al., 1979). We tested for this possibility by measuring the Ca channel reversal potential under conditions that might promote such depletion and affect the reversal potential in our preparations, as has been reported for similar experiments in other cardiac preparations (Bassingthwaighte and Reuter, 1972).

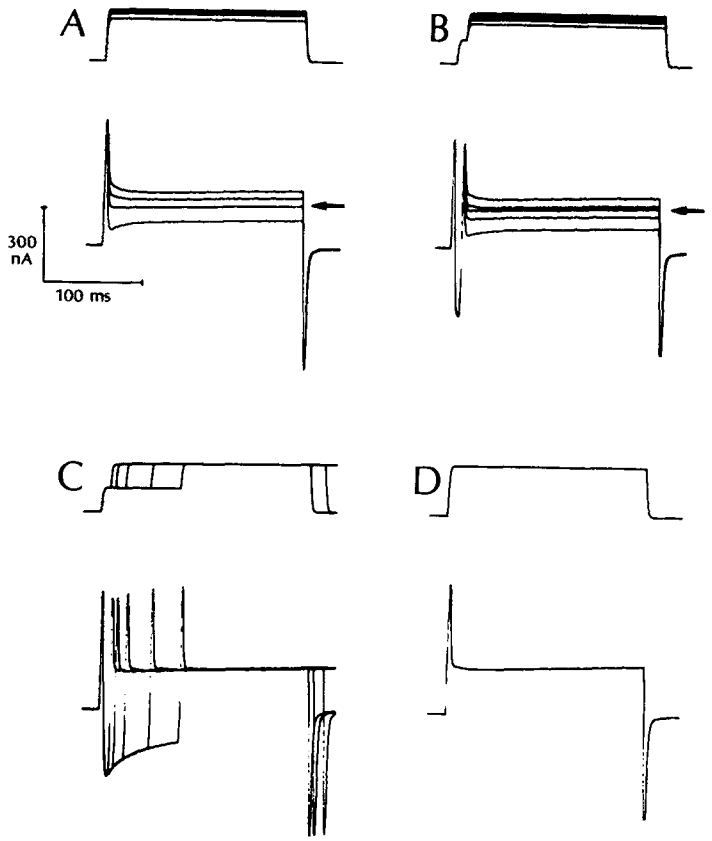

FIGURE 4. Tests for depletion of charge carrier. (*A*) Current records are shown in response to pulses to +41, +51, +56, and +58 mV. Current reversed (arrow) near +50 mV. (*B*) Current records shown in response to voltage pulses to +41, +45, +49 (V_{rev}, arrow), +51, and +54 mV after 10-ms prepulses to +5 mV. (*C*) Superposition of current traces recorded during test pulses to +51 mV after prepulses of variable duration (10, 25, 50, and 80 ms) were imposed to +5 mV. (*D*) Membrane current recorded during a single pulse to +51 mV. The holding potential was −42 mV in all experiments. 5.4 mM Sr Tyrode solution. Preparation 308-3.

Fig. 4 shows an example of an experiment designed to test for depletion when Sr^{2+} is the permeant divalent cation. We chose Sr^{2+} as the charge carrier because it is more permeant than Ca^{2+} (Hess et al., 1983; Hagiwara and Byerly, 1981) and is more likely to cause depletion because of the larger current that it promotes through the channel. The figure shows measurement of the reversal potential (using net current records) under several conditions. The reversal potential was found to be near +50 mV by applying a series of depolarizing voltage steps from a −42-mV holding potential (*A*). This procedure also showed that peak inward current was measured at a potential near +5 mV. We then applied brief prepulses to +5 mV to promote large surges of inward current and repeated the reversal potential measurements (*B*). The reversal potential following the prepulse remained at +50 mV. Finally, we interrupted voltage pulses to +5 mV at different

times by voltage steps to +50 mV, the measured reversal potential. Currents measured during this protocol (*C*) were compared with currents measured during a single step to V_{rev} (*D*). We detected no change in V_{rev} during any of these measurements in this and three other preparations. We conclude that the time dependence of Ca channel current in these experiments is not caused by changes in the extracellular ion concentration. Our results are consistent with reports of Ca channel current inactivation in single cardiac cells (e.g., Isenberg and Klockner, 1982; Lee and Tsien, 1982), where decay of inward current is not due to ion depletion.

KINETICS OF CHANNEL INACTIVATION: ONSET OF INACTIVATION Fig. 5 illus-

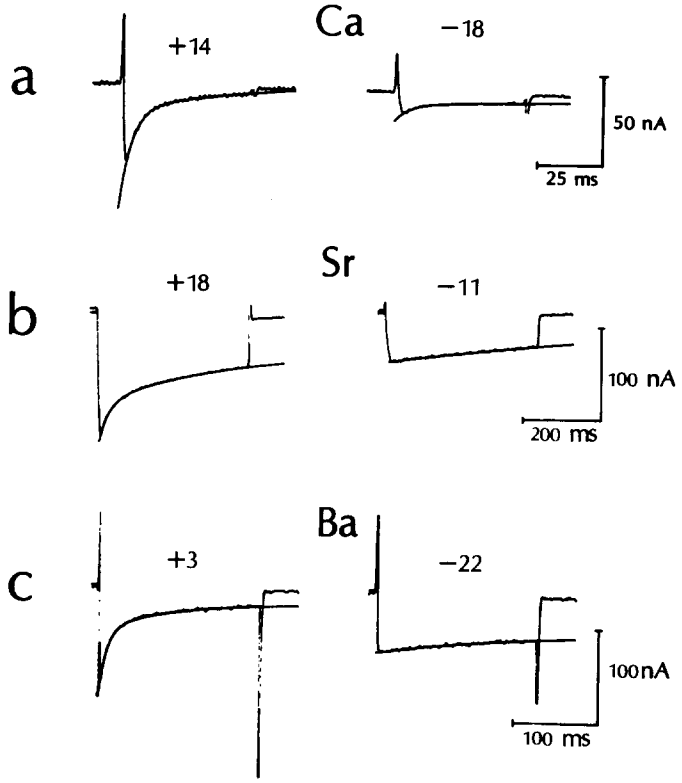

FIGURE 5. Time course of Ca, Sr, and Ba current inactivation during depolarizing voltage pulses. The time dependence of membrane current was analyzed after subtracting off background current measured in the presence of nisoldipine (10 μM) for Ca and Sr current. Experimentally measured membrane current is shown superimposed on curves returned by the fitting routine (Methods). (*a*) Ca current. Left panel: pulse voltage, +14 mV; τ_1 = 5 ms; τ_2 = 60 ms. Right panel: pulse voltage, −18 mV; τ_1 = 5 ms; τ_2 = 47 ms. 5.4 mM Ca; HP, −63 mV. Preparation 292-2. (*b*) Sr current. Left panel: pulse voltage, +18 mV; τ_1 = 13 ms; τ_2 = 155 ms. Right panel: pulse voltage, −11 mV; τ_1 = 94 ms; τ_2 = 744 ms. HP, −50 mV; 5.4 mM Sr Tyrode solution. Preparation 301-1. (*c*) Ba current. Left panel: pulse voltage, +3 mV; τ_1 = 14 ms; τ_2 = 164 ms. Right panel: pulse voltage, −22 mV; τ_1 = 152 ms; τ_2 = 996 ms. HP, −53 mV; 5.4 mM Ba Tyrode solution. Preparation 311-3.

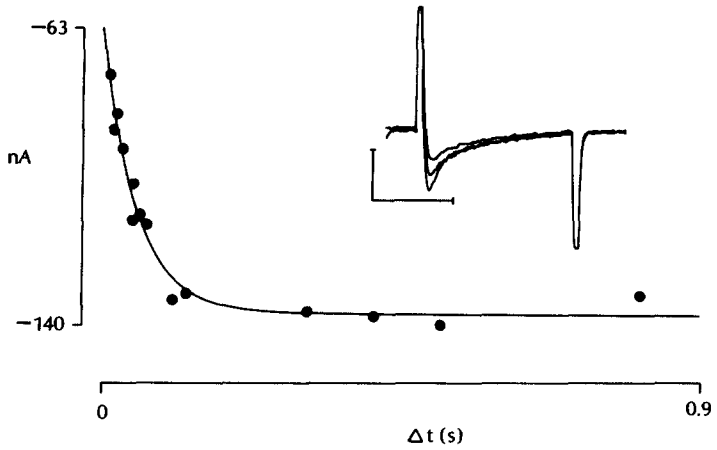

FIGURE 6. Time course of recovery from inactivation of Ca current after a brief prepulse. Membrane potential was stepped to −14 mV for 100 ms to inactivate some of the Ca channels. The inset shows currents recorded during test pulses to 0 mV after returning to −60 mV for 20, 50, and 800 ms. The time constants of inactivation of the currents shown in the inset (τ_1, τ_2): 5.5 and 51 ms (after 20 ms); 4.3 and 32 ms (after 50 ms); and 3.2 and 26.2 ms (after 800 ms). Calibration bars: 100 nA, 25 ms. Peak current, measured during each test pulse, is plotted against time at −60 mV. The best fit to these data (curve) was obtained with a single-exponential function (τ = 50 ms). 5.4 mM Ca Tyrode solution. Preparation 292-1.

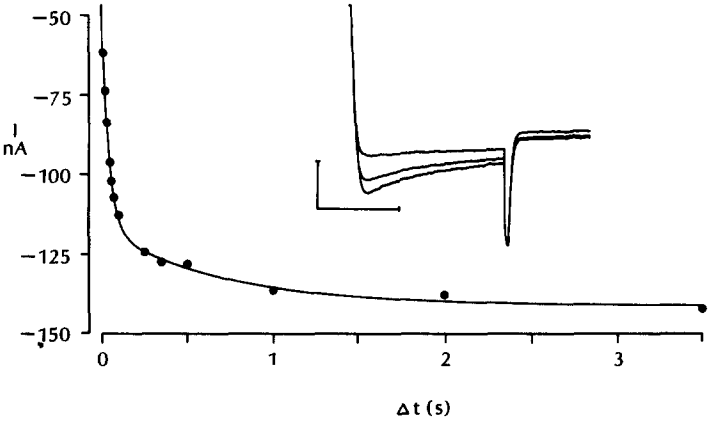

FIGURE 7. Time course of recovery from inactivation of Sr current after a prepulse that promotes biphasic recovery. Similar protocol to that used in the experiment of Fig. 8, but prepulse was applied to −1 mV for 250 ms to inactivate the channels. Recovery was measured by imposing test pulses to +2 mV after variable periods at −48 mV. The inset shows current measured after 10, 100, and 2,000 ms at −48 mV. The time constants of inactivation of the currents shown in the inset: 29 (after 10 ms), 23 (after 100 ms), and 23 ms (after 2 s). Calibration bars: 100 nA, 25 ms. Peak inward test current was plotted against recovery time at −48 mV. Curve: best fit to data by a function with two time constants (τ_1 = 43 ms; τ_2 = 700 ms). 5.4 mM Sr Tyrode solution. Preparation 310-1.

trates the analysis of the time-dependent decay of Ca channel current that was observed during depolarizing voltage steps in Ca-, Sr-, or Ba-containing solutions. For Ca and Sr currents, membrane current was measured before and after blocking Ca current with nisoldipine (10 μM) to determine and subtract off background current. The drug-sensitive current traces (Ca and Sr) and total current (Ba) were then fitted to a two-exponential function (Methods). The figure shows examples of the determination of the time dependence of currents recorded in response to two voltages for each charge carrier. In the case of each voltage, current and the best-fit curve determined by the fitting procedure are superimposed to illustrate the agreement between the fitted function and the experimental records. When Ca currents are analyzed in this manner (Fig. 5*a*), the time constants of inactivation rate are found to be fast ($\tau_1 \leq 10$ ms; $\tau_2 \leq 100$ ms) and show little variation with membrane potential (see Fig. 8, circles).

Sr (*b*) and Ba (*c*) currents inactivate very slowly during voltage steps to potentials more negative than −10 mV, but decay much faster at more positive potentials (compare right and left columns). As was the case for Ca currents, the inactivation of Ba and Sr currents was best fit by functions with two exponentials. This current clearly inactivates when either Ba^{2+} or Sr^{2+} is the principal charge carrier and the time course of inactivation is steeply voltage dependent (see Fig. 8). In the presence of Sr or Ba, time constants for the slower phase of inactivation (τ_2) were too long at test voltages between −10 and −25 mV to be accurately determined with 200-ms pulse durations. Therefore, some experiments were carried out with longer-duration pulses (500 ms, 1 s) to confirm the results obtained with briefer pulses. These results are included in the data of Fig. 8.

Recovery from Inactivation

We next investigated the time course of recovery from inactivation in solutions containing Ca, Ba, or Sr as the charge carrier. The data analyzed during depolarizing voltage steps consistently indicated that inactivation was better described by a two-exponential process in each solution, so the recovery from inactivation experiments was designed to test for the possibility of a two-exponential process in this case as well.

Fig. 6 shows the results of an experiment designed to study the recovery from inactivation that develops during brief depolarizations in Ca-containing solutions. Conditioning pulses were applied to −14 mV for 100 ms to promote fast inactivation of the channels. The membrane was then returned to a −60-mV holding potential for variable intervals to allow for recovery from inactivation before applying test pulses to 0 mV to measure Ca current. Peak inward current measured during the test pulse (inset) was plotted against the recovery interval and the resulting curve was fitted to an exponential function. For brief prepulses ($\leq$100 ms), the recovery curve is best fitted by a single-exponential function. This result is shown for Ca currents but was also found to be the case for Ba and Sr currents.

When similar experiments are carried out with longer prepulses ($\geq$250 ms), recovery from inactivation (in all solutions) is characterized by fast and slow phases. An example of the biphasic recovery of Sr current is shown in Fig. 7.

Data from all of our experiments designed to investigate the kinetics of

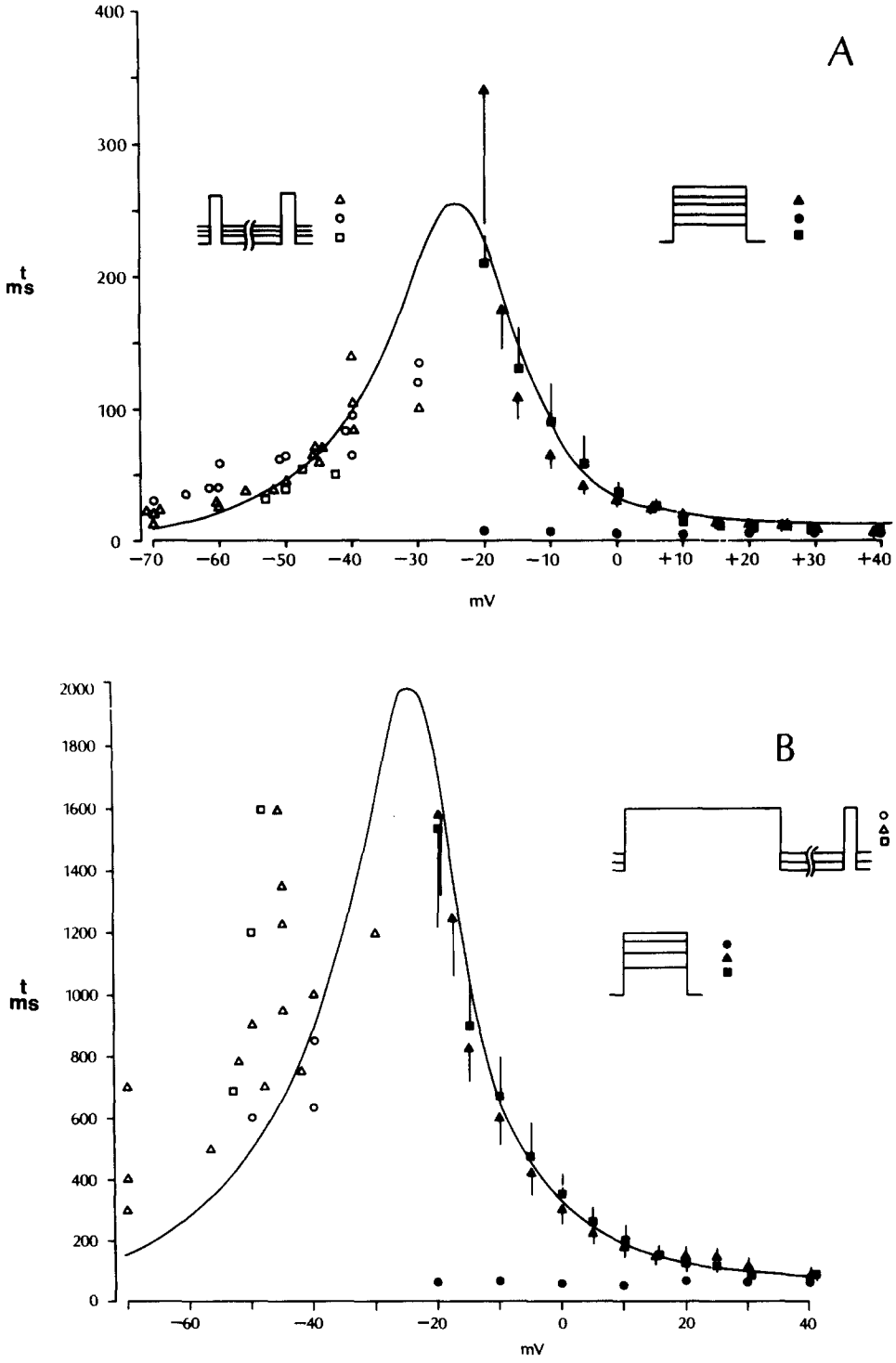

inactivation are summarized in Fig. 8. Data for recovery from inactivation (open symbols) were obtained at voltages negative to −40 mV and data for the onset of inactivation were determined at voltages positive to −30 mV (filled symbols). The time course of recovery from inactivation is insensitive to changes in the permeant divalent cation, but there is a marked change in the voltage dependence of the onset of inactivation rate when Sr or Ba replaces Ca_o. The smooth curves in the figure were generated by a model for voltage-dependent inactivation (described in the Discussion) that was fit to the onset rates for Ba and Sr currents. The data in Fig. 8 were obtained at 37°C. When the temperature was lowered, the inactivation time constants recorded for Ba and Sr currents were prolonged (approximate $Q_{10} = 2.5$).

Steady State Availability of Ca Channel Current

One observation that has led to the hypothesis of Ca_i-mediated Ca channel inactivation in previous studies is that inactivation produced by a depolarizing prepulse varies with Ca entry during that pulse (see Introduction). Marban and Tsien (1981) have reported this phenomenon in calf Purkinje fibers in which outward currents had been blocked by Cs loading when Ca^{2+} but not Ba^{2+} was the permeant divalent cation. We have done similar experiments comparing inactivation curves obtained in Sr- and Ca-containing solutions.

In the majority of our preparations ($n = 11$), when we used 500-ms conditioning voltage pulses, we found little change in the amount of Ca current inactivated as the conditioning pulse was made progressively more positive than +10 mV. The inactivation curves measured in these experiments could be well fit by an expression of the form $[1 + \exp(V - V_h/k)]^{-1}$ with the following parameters: $V_h = -22.2 \pm 0.17$, $k = 4.99 \pm 0.07$. However, in one experiment, we did observe a decrease in inactivation as the conditioning pulse voltage approached +60 mV, but the amount of current recovered by this change in prepulse voltage represented only ~20% of the current that inactivated. The result of this experiment is qualitatively consistent with previous reports for Ca_i-mediated inactivation (Marban and Tsien, 1981; Tillotson, 1979), but the magnitude of this effect in our experiments is small and occurs infrequently.

When we repeated this experiment for Sr currents, the 500-ms inactivation curve also did not show any decrease in inactivation as the conditioning pulse voltage was increased beyond 0 mV. This is similar to results reported by Marban

FIGURE 8. (*opposite*) Time course of inactivation: cumulative data. Time constants obtained from the fitting procedure (Methods) are plotted for recovery from (open symbols) and onset of (filled symbols) inactivation. Data are shown for Ca (circles, $n = 10$), Sr (triangles, $n = 9$–10), and Ba (squares, $n = 7$) currents. Data for onset of inactivation are plotted as mean ± SEM. Individual time constants are plotted for recovery from inactivation. The theoretical curves plotted in the figure were generated using Eqs. 7 and 8 of Chiu (1977) with the following rate constants (ms^{-1}): $a_{10} = (0.00048)(\exp[-(V + 4)/12])$; $a_{01} = (0.065)/(1 + \exp[-(V)/6])$, $a_{12} = (0.0065)/[1 + \exp(-V/8)]$, and $a_{21} = (0.00008)(\exp[-(V - 5)/17])$. (*A*) Time constants for fast phase of inactivation. (*B*) Time constants for slower phase of inactivation.

and Tsien (1981) for Ba currents. Since the inactivation kinetics for Sr and Ba currents differ from Ca currents (see Fig. 8), it is possible that this conditioning pulse duration might be too short to fully inactivate Sr current, but Fig. 9 shows that increasing the prepulse duration does not change the shape of the inactivation curve at more positive prepulse potentials.

Influence of External Surface Change

We have compared steady state activation data for Sr and Ca currents in the Purkinje fiber to test for the possibility that modification of surface charge accounts for the differences that we observe in the inactivation kinetics of these currents. We chose to compare activation curves because of the difficulties in adjusting prepulse durations for comparison of steady state inactivation data (see Fig. 9 and Discussion).

Fig. 10 compares steady state activation data obtained in Sr- and Ca-containing solutions. In each case, we measured membrane current during a series of voltage pulses applied from a common holding potential in the absence and presence of nisoldipine. Background current was subtracted, and the resulting current records were fitted to exponential functions that were extrapolated to the beginning of these pulses. This procedure relies on the assumption that activation is much faster than inactivation during a test pulse, an assumption supported by studies using single cardiac cells (Lee and Tsien, 1982). The extrapolation is then a measure of current after activation has reached steady state at the test pulse voltage, but when inactivation remains unchanged from conditions at the holding

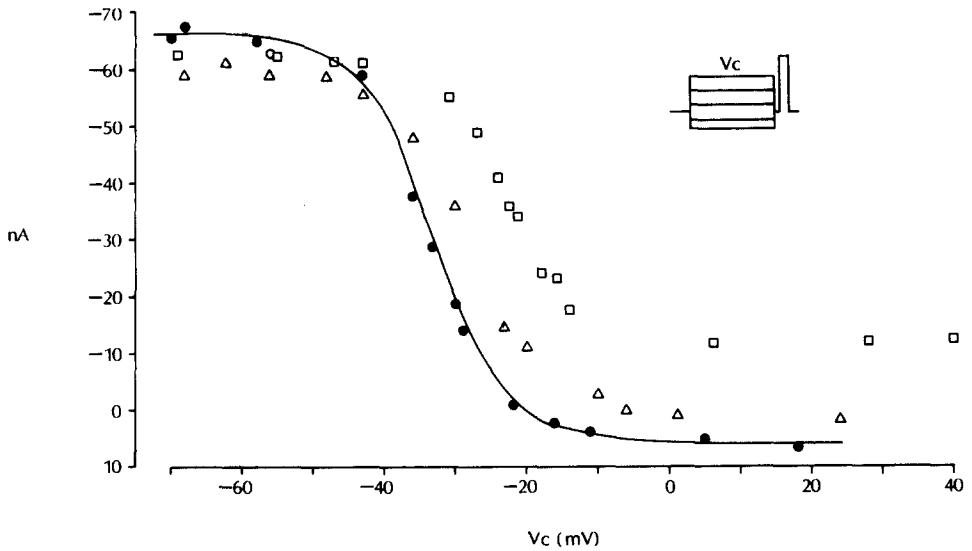

FIGURE 9. Effect of prepulse duration on Sr current inactivation curve. Prepulse duration was varied, and test current was measured at +2 mV. Peak inward test currents are plotted against prepulse potential for prepulse durations of 100 ms (□), 500 ms (△), and 2 s (●). The smooth curve has a half-maximal voltage of −33.3 mV. HP, −56 mV; 5.4 mM Sr Tyrode solution. Preparation 316-1.

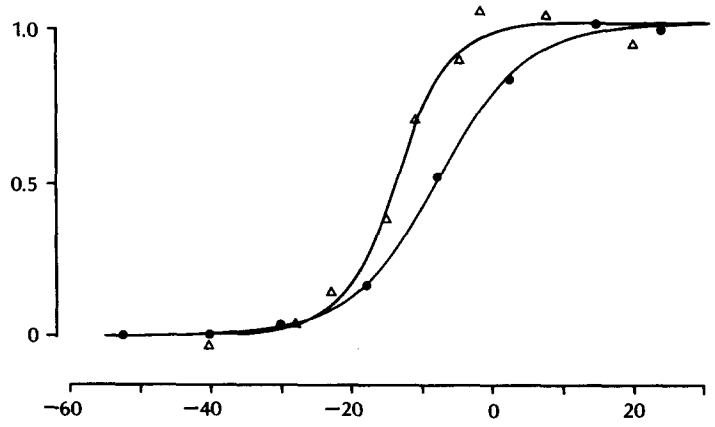

FIGURE 10. Steady state activation curves recorded in Sr- and Ca-containing solutions. See text for details of measurements. The curves in each panel are of the form of $d_\infty = (1 + \exp[-(V - V_h)/k])^{-1}$. Parameters for this curve in each solution are the best fit of this function to the data (Methods). (●) Activation curve measured in 5.4 mM Ca Tyrode solution: $V_h = -8$ mV; $k = 6.1$ mV. Preparation 292-1. (△) Activation curve measured in 5.4 mM Sr Tyrode solution: $V_h = -13.7$ mV; $k = 3.8$ mV. The ordinate is normalized current. The abscissa is membrane potential in millivolts. Preparation 295-2.

potential. The reversal potential measured for each experiment was used to determine conductances, and the activation parameter (d_∞) (see Reuter, 1979) was obtained by normalizing these data to the maximal conductance.

In the experiments shown in Fig. 10, we measured a $V_{1/2}$ of −13.7 mV for the steady state activation curve (in 5.4 mM Sr, triangles). This is typical of all of our experiments in Sr solutions in which we determined $V_{1/2}$ to be -11.1 ± 3.7 mV ($n = 7$), and is ~5 mV more negative than the value for this parameter measured in 5.4 mM Ca^{2+} solution (Fig. 10, circles).

DISCUSSION

Evidence for a Voltage-dependent Inactivation Mechanism

SR AND BA CURRENTS Properties of Ca channel current inactivation in the Purkinje fiber resemble those used to identify voltage-dependent inactivation mechanisms in the Ca channels of other cells. Inactivation of Purkinje fiber Ca channel current persists when Ca_o is replaced by Ba or Sr, and the rates of inactivation are very similar when Ba^{2+} or Sr^{2+} is the principal charge carrier. This is true for both onset of and recovery from inactivation. Increasing the prepulse depolarization toward the expected reversal potential of the channel does not reduce the degree or rate of inactivation of Sr or Ba currents. Thus, the inactivation of Ca channel current is not proportional to the magnitude of the current flowing through the channel when Ba or Sr carries the charge. Similar properties have supported the interpretation of a voltage-dependent inactivation mechanism for Ca current in eggs from the polycheate *Neanthes*

arenaceodentata (Fox, 1981; Fox and Krasne, 1981) and mouse myeloma cells (Fukushima and Hagiwara, 1983).

Evidence for a Ca-dependent Mechanism

It has been suggested by others (Marban and Tsien, 1981; Hume and Giles, 1982; Mentrard et al., 1984) that Ca current inactivation in a variety of cardiac cells is mediated, at least in part, by Ca ions. The principal evidence for this interpretation has come from the relationships between Ca entry during a conditioning pulse and Ca current inactivation during a subsequent test pulse, as first described in molluscan neurons by Tillotson (1979) and Eckert and Tillotson (1981). It thus seemed reasonable that a Ca-mediated process might underlie some of the marked differences we observed between inactivation of Ca^{2+} and Sr^{2+} (or Ba^{2+}) currents.

The strongest evidence for a Ca-mediated inactivation mechanism in our experiments comes from the kinetic data. Replacement of Ca_o by either Ba or Sr greatly slows the onset of inactivation, particularly at voltages between −20 and +10 mV. In addition, when Ca^{2+} is the permeant ion, the time course of inactivation is very insensitive to changes in membrane potential (voltage −30 mV or greater), in contrast to the data recorded in Ba or Sr solutions.

We considered the possibility that these changes in kinetics might be due to changes in external surface charge when Ba or Sr replaced Ca_o. Changes in external surface charge are known to shift voltage-dependent gating processes along the voltage axis, and these shifts occur for both activation and inactivation parameters (Wilson et al., 1983; Begenisich, 1975; Frankenhaeuser and Hodgkin, 1957; Weidmann, 1955). Our data for activation curves, which show only small changes when Sr replaces Ca_o (Fig. 10), as well as for time constants of recovery from inactivation (Fig. 8), suggest that external surface charge changes are too small to account for the differences between Ca and Sr (or Ba) current inactivation.

Another possibility is that Ca, but not Sr or Ba, binds to sites on the cytoplasmic side of the membrane, causing a voltage shift of the intrinsic voltage-dependent mechanism in the negative direction (Tsien, 1983; Eckert and Tillotson, 1981). Although our data do not rule out such a mechanism, they do place constraints on it: (*a*) the binding to these sites must occur only during depolarizing steps that cause inward surges of Ca^{2+}, and (*b*) the voltage shifts caused by this binding must be on the order of −60 mV if they are to account for the data of Fig. 8.

Inactivation: a Combined Mechanism

We interpret these results as evidence that Ca channel current in the Purkinje fiber inactivates by a mechanism that is both voltage dependent and Ca dependent. In this view, inactivation of Ba or Sr currents reflects a voltage-dependent mechanism. This mechanism is somehow modulated by Ca entry during depolarizing voltage steps when Ca^{2+} is the divalent charge carrier. This modulation is most apparent in the contrast between the time course of inactivation measured during voltage pulses between −20 and 0 mV for Ca and Sr (or Ba) currents (Fig. 8). In this voltage range, Ca entry during the depolarization may speed the decay of Ca current. However, at voltages more positive than 0 mV, the rates of

inactivation for currents carried by all charge carriers converge. This suggests that at positive potentials the kinetics of a voltage-dependent process become sufficiently fast to make them indistinguishable from a Ca-mediated mechanism.

The data shown in Figs. 6 and 7 also support the interpretation that Ca entry can affect the time course of inactivation. The insets of these figures show Ca (Fig. 6) and Sr (Fig. 7) currents measured at common voltages after different intervals at a potential that promoted recovery after an inactivating conditioning voltage pulse. When Sr carries the charge (Fig. 7), the time course of current decay during each of the three traces shown is not systematically changed as the current magnitude increases. In contrast, when Ca carries the charge (Fig. 6), the time course of current decay during the test pulses is progressively faster as the interpulse interval is increased. Thus, the inactivation rate for Ca, but not Sr, current is affected by current magnitude despite the fact that voltage is constant. This behavior is not predicted by a purely voltage-gated inactivation process (also see Mentrard et al., 1984).

The rates of recovery from inactivation in our experiments are very similar for Ba, Sr, and Ca currents at membrane potentials more negative than −40 mV (Fig. 8). According to the interpretation of a combined inactivation mechanism, these recovery times might reflect the repriming of a common voltage-dependent gating mechanism, because no inward current flows at these recovery potentials. An alternative interpretation, suggested for Ca channels in *Aplysia* neurons (Eckert et al., 1981) and frog heart cells (Mentrard et al., 1984), is that recovery from inactivation follows the time course of removal of Ca^{2+} from the cytoplasm. We cannot rule out this possibility in our experiments, but if such a mechanism underlies the recovery kinetics we observe, then the time course of removal of Sr and Ba must be the same as the removal of Ca, and the removal mechanism must be steeply voltage dependent (Fig. 8).

Our observations in the calf Purkinje fiber resemble those of A. M. Brown et al. (1981) in snail neurons. The presence of both mechanisms in cardiac tissue would unify several recent reports that have suggested voltage-dependent (Campbell et al., 1983; Lee and Tsien, 1982; Reuter et al., 1982; Fischmeister et al., 1981) or Ca-mediated (Hume and Giles, 1982; Marban and Tsien, 1981; Fischmeister et al., 1981; H. F. Brown et al., 1981) inactivation mechanisms in different cardiac cells.

Voltage Dependence of Inactivation: Comparison with Previous Studies

We observe that the relaxation of Ca channel current measured during depolarizing voltage pulses is described by a two-exponential process in the Purkinje fiber, and this finding is independent of the divalent charge carrier. Similar observations have been made in enzymatically dispersed bovine ventricular myocytes (Isenberg and Klockner, 1982) and in snail neurons (A. M. Brown et al., 1981). However, in contrast to Isenberg and Klockner (1982), we find that recovery from inactivation is also characterized by two time constants in a manner that depends on the duration of the conditioning prepulse (see Figs. 7 and 8).

Because of the complexity of the inactivation mechanisms in this channel, it is not surprising that previous reports of its inactivation kinetics in cardiac prepa-

rations are somewhat variable (for review, see Reuter, 1979). We find that both the fast and slow time constants of Ca, Ba, and Sr current inactivation reach maxima near −25 mV and decrease with depolarization. These results are consistent with voltage-clamp analyses of current in isolated ventricular cells (Isenberg and Klockner, 1982), but earlier sucrose-gap voltage-clamp studies in other multicellular cardiac preparations (Rueter and Scholz, 1977; McDonald and Trautwein, 1978; Kohlhardt et al., 1975) have indicated that the time constants of inactivation increase continuously for voltages more positive than −30 mV.

Significance of the Reversal Potential Measurements

Our observation that the Ca channel current reversal potential remains stable under extreme experimental conditions (Fig. 4) contrasts with previous results obtained in sheep ventricular muscle (Bassingthwaighte and Reuter, 1972). Our confidence in the accuracy of our measurements of E_{rev} is restricted to a range of ±3 mV because time-dependent currents become very small as V_m approaches V_{rev}. Bassingthwaighte and Reuter (1972) reported changes in E_{rev} on the order of 22 mV for similar experiments in a sheep ventricular trabeculae preparation.

In our experiments, it is worth asking how much the reversal potential would change if depletion of external divalent cations caused the changes in inward current that we measured. For example, in the experiment shown in Fig. 4, inward current measured at +5 mV decreased roughly by a factor of 2 in 80 ms. Using the theory of Fatt and Ginsborg (1958) as described by Junge (1976), we can estimate that about a twofold change in $[Sr]_o$ would be necessary to cause a twofold decrease in inward current. If $[Sr]_o$ were decreased by a factor of 2 by depletion, then the reversal potential (at 37°C) would be expected to change by 9 mV. This is a significantly larger change in E_{rev} than the 3-mV determination error we observe. Thus, we conclude that in the calf Purkinje fiber, depletion of charge carrier from a restricted extracellular space could at most produce a small change in V_{rev} and thus cannot account for the time course of relaxation of current during depolarizing voltage steps in our study.

Voltage-dependent Inactivation: Models

Since Ca entry appears to modulate the conductance of the Ca channel, our data suggest that it is more straightforward to analyze Ba or Sr currents in order to investigate properties of Ca channel current that might be modulated by membrane potential. We thus analyzed the Ba and Sr data using a three-state model for the inactivation process in which transitions proceed from one open to two closed states:

$$\begin{array}{ccccc} \text{OPEN} & & \text{CLOSED} & & \text{CLOSED} \\ 0 & \underset{a_{10}}{\overset{a_{01}}{\rightleftharpoons}} & 1 & \underset{a_{21}}{\overset{a_{12}}{\rightleftharpoons}} & 2 \end{array}$$

The equations describing the occupancy of each of these states, along with the general solution for the functional occupancy of the open state as described by Chiu (1977), were used to estimate rate constants for the transitions that are consistent with the steady state inactivation curves (Fig. 9) and the onset of

inactivation kinetic data (Figs. 5 and 8). These rate constants were then used to compute time constants for recovery from inactivation as well as onset of inactivation, and these time constants are plotted as the smooth curves in Fig. 8, *A* and *B*.

The model predicts a bell-shaped curve for both the fast and slow inactivation time constant-voltage relation for Ba and Sr currents. This curve resembles comparable curves for Na current in squid axons (see Meves, 1978). The data for recovery from inactivation (voltages less than −40 mV) are well fit by this curve, even though the parameters for the curve were obtained from the onset of inactivation data. This supports the interpretation that Ba and Sr current inactivation is a voltage-dependent mechanism. In addition, the recovery from inactivation of Ca current is described by this curve, but the onset of inactivation, where Ca entry causes more rapid inactivation, is not. Thus, it is not surprising that previous experiments designed to investigate the relationship between the onset and recovery of inactivation of Ca currents have yielded variable results (Shimoni, 1981; McDonald and Trautwein, 1978; Kohlhardt et al., 1975; Gettes and Reuter, 1974) and have led to speculation on the existence of separate onset and recovery processes (Kohlhardt et al., 1975).

Although this model satisfactorily describes the time constant vs. voltage data, it has two serious weaknesses and thus must not be considered the only possible scheme that accounts for our data. The first problem is that the rate constants are determined, in part, by steady state inactivation data. As shown in Fig. 9, the shape of the inactivation curve is altered when the prepulse duration is increased. This is due in part to the nature of the time constants of the inactivation mechanisms explored in this study, but it is also due to the very slow inactivation that affects Ca channel current with prolonged depolarization (Scheuer, 1983; Kass and Scheuer, 1982). Thus, it is very difficult to extract an inactivation curve reflecting steady state inactivation for the processes described in this study while excluding contributions from very slow inactivation.

The second problem with this model, which assumes that the forward rate constants (a_{01}, a_{12}) dominate at positive potentials, is that it fails quantitatively in its description of the relaxation of Ca channel current during voltage steps. The model predicts that as voltages are made more positive, the ratio of fast to total inactivating current should increase and approach unity at voltages of >10 mV. Our data display this trend, but this ratio never exceeds 0.8. We explored other models for inactivation, such as a system with two independent subunits (Chandler and Meves, 1970), but were not able to improve the fit to our data. A possible explanation for this difference is that these data reflect two populations of Ca channels, but verification of such a possibility must wait for support from single channel recordings.

Original version received 19 December 1983 and accepted version received 11 June 1984.

REFERENCES

Attwell, D., D. Eisner, and J. Cohen. 1979. Voltage-clamp and tracer flux data: effects of a restricted extracellular space. *Q. Rev. Biophys.* 12:213–261.

Bassingthwaighte, J. B., and H. Reuter. 1972. Calcium movements and excitation-contraction

coupling in cardiac cells. *In* Electrical Phenomena in the Heart. W. C. DeMello, editor. Academic Press, Inc., New York. 353–395.

Begenisich, T. 1975. Magnitude and locations of surface charges on *Myxicola* giant axons. *J. Gen. Physiol.* 66:47–65.

Bers, D. M. 1983. Depletion of Ca_o during cardiac muscle twitches measured with Ca selective microelectrodes: Ca influx during single beats. *Biophys. J.* 41:150*a*. (Abstr.)

Bevington, P. R. 1969. Data Reduction and Error Analysis for the Physical Sciences. McGraw-Hill Book Co., New York. 336 pp.

Brown, A. M., K. Morimoto, Y. Tsuda, and D. L. Wilson. 1981. Calcium current-dependent and voltage-dependent inactivation in *Helix aspersa*. *J. Physiol. (Lond.)*. 320:193–218.

Brown, H. F., J. Kimura, and S. Noble. 1981. Calcium entry dependent inactivation of the slow inward current in the rabbit sinoatrial node. *J. Physiol. (Lond.)*. 320:11P. (Abstr.)

Campbell, D. L., K. Robinson, and W. Giles. 1983. Voltage-dependent inactivation-reactivation of TTX-resistant inward current in single cells from bullfrog atrium. *Biophys. J.* 41:311*a*. (Abstr.)

Chandler, W. K., and H. Meves. 1970. Slow changes in membrane permeability and long-lasting action potentials in axons perfused with fluoride solutions. *J. Physiol. (Lond.)*. 211:707–728.

Chiu, S. Y. 1977. Inactivation of sodium channels: second order kinetics in myelinated nerve. *J. Physiol. (Lond.)*. 273:573–596.

Coraboeuf, E. 1980. Voltage clamp studies of the slow inward current. *In* The Slow Inward Current and Cardiac Arrhythmias. D. P. Zipes, J. C. Bailey, and V. Elharrar, editors. Martinus Nijhoff, The Hague. 25–95.

Dresdner, K., R. P. Kline, and J. Kupersmith. 1982. Extracellular calcium ion depletion in frog ventricle. *Biophys. J.* 37:293*a*. (Abstr.)

Eckert, R., and D. L. Tillotson. 1981. Calcium-mediated inactivation of the calcium conductance in caesium-loaded giant neurones of *Aplysia californica*. *J. Physiol. (Lond.)*. 314:265–280.

Eckert, R., D. Tillotson, and P. Brehm. 1981. Calcium-mediated control of Ca and K currents. *Fed. Proc.* 40:2226–2232.

Fatt, P., and B. L. Ginsborg. 1958. The ionic requirements for the production of action potentials in crustacean muscle fibres. *J. Physiol. (Lond.)*. 142:516–543.

Fischmeister, R., D. Mentrard, and G. Vassort. 1991. Slow inward current inactivation in frog heart atrium. *J. Physiol. (Lond.)*. 320:27–28P. (Abstr.)

Fox, A. P. 1981. Voltage-dependent inactivation of a calcium channel. *Proc. Natl. Acad. Sci. USA*. 78:953–956.

Fox, A. P., and S. Krasne. 1981. Two calcium currents in egg cells. *Biophys. J.* 33:145*a*. (Abstr.)

Fozzard, H. A., and M. Hiraoka. 1973. The positive dynamic current and its inactivation properties in cardiac Purkinje fibers. *J. Physiol. (Lond.)*. 234:569–586.

Frankenhaeuser, B., and A. L. Hodgkin. 1957. The action of calcium on the electrical properties of squid axons. *J. Physiol. (Lond.)*. 137:218–244.

Fukushima, Y., and S. Hagiwara. 1983. Voltage-gated calcium channels in mouse myeloma cells. *Biophys. J.* 41:292*a*. (Abstr.)

Gettes, L. S., and H. Reuter. 1974. Slow recovery from inactivation of inward currents in mammalian myocardial fibers. *J. Physiol. (Lond.)*. 240:703–724.

Hagiwara, S., and L. Byerly. 1981. Calcium channel. *Annu. Rev. Neurosci.* 4:69–125.

Hess, P., K. S. Lee, and R. W. Tsien. 1983. Ion-ion interactions in the Ca channel of single heart cells. *Biophys. J.* 41:293*a*. (Abstr.)

Hilgemann, D. W., M. Delay, and G. A. Langer. 1983. Measurement of activation-related cumulative depletions of free extracellular calcium in guinea pig atrium with antipyrylazo III. *Circ. Res.* 53:779–794.

Hume, J. R., and W. Giles. 1982. Turn-off of a TTX-resistant inward current "i_{Ca}" in single bullfrog atrial cells. *Biophys. J.* 37:240*a*. (Abstr.)

Isenberg, G., and U. Klockner. 1982. Calcium currents of isolated bovine ventricular myocytes are fast and of large amplitude. *Pflügers Arch. Eur. J. Physiol.* 395:30–41.

Junge, D. 1976. Nerve and Muscle Excitation. Sinauer Associates, Sunderland, MA. 143 pp.

Kass, R. S. 1982. Nisoldipine: a new, more selective calcium current blocker in cardiac Purkinje fibers. *J. Pharmacol. Exp. Ther.* 223:446–456.

Kass, R. S., and T. Scheuer. 1982. Slow inactivation of calcium channels in the cardiac Purkinje fiber. *J. Mol. Cell. Cardiol.* 14:615–618.

Kass, R. S., T. Scheuer, and K. J. Malloy. 1982. Block of outward current in cardiac Purkinje fibers by injection of quaternary ammonium ions. *J. Gen. Physiol.* 79:1041–1063.

Kass, R. S., S. A. Siegelbaum, and R. W. Tsien. 1979. Three-micro-electrode voltage clamp experiments in calf cardiac Purkinje fibers: is slow inward current adequately measured? *J. Physiol. (Lond.).* 290:201–225.

Kohlhardt, M., H. Krause, M. Kubler, and A. Herdey. 1975. Kinetics of inactivation and recovery of the slow inward current in the mammalian ventricular myocardium. *Pflügers Arch. Eur. J. Physiol.* 355:1–17.

Lee, K. S., and R. W. Tsien. 1982. Reversal of current through calcium channels in dialyzed single heart cells. *Nature (Lond.).* 297:498–501.

Marban, E., and R. W. Tsien. 1981. Is the slow inward calcium current of heart muscle inactivated by calcium? *Biophys. J.* 33:143*a*. (Abstr.)

Marban, E., and R. W. Tsien. 1982. Effects of nystatin-mediated intracellular ion substitution on membrane currents in calf Purkinje fibres. *J. Physiol. (Lond.).* 329:569–587.

Marquardt, D. W. 1963. An algorithm for least-squares estimation of nonlinear parameters. *J. Soc. Ind. Appl. Math.* 11:431–441.

McDonald, T. F., and W. Trautwein. 1978. Membrane currents in cat myocardium: separation of inward and outward components. *J. Physiol. (Lond.).* 274:193–216.

Mentrard, D., G. Vassort, and R. Fischmeister. 1984. Calcium-mediated inactivation of the calcium conductance in cesium-loaded frog heart cells. *J. Gen. Physiol.* 83:105–131.

Meves, H. 1978. Inactivation of the sodium permeability in squid giant nerve fibers. *Prog. Mol. Biol.* 33:207–230.

Reuter, H. 1979. Properties of two inward membrane currents in the heart. *Annu. Rev. Physiol.* 41:413–424.

Reuter, H., and A. Scholz. 1977. A study of the ion selectivity and the kinetic properties of the calcium dependent slow inward current in mammalian cardiac muscle. *J. Physiol. (Lond.).* 264:17–47.

Reuter, H., C. F. Stevens, R. W. Tsien, and G. Yellen. 1982. Properties of single calcium channels in cultured cardiac cells. *Nature (Lond.).* 297:501–504.

Scheuer, T. 1983. Calcium current in Purkinje fibers: effects of slow inactivation and diphenylhydantoin. Ph.D. Thesis. University of Rochester, Rochester, NY.

Shimoni, Y. 1981. Parameters affecting the slow inward channel repriming process in frog atrium. *J. Physiol. (Lond.).* 320:269–291.

Siegelbaum, S. A., and R. W. Tsien. 1980. Calcium-activated outward current in calf cardiac Purkinje fibers. *J. Physiol. (Lond.).* 299:485–506.

Tillotson, D. 1979. Inactivation of Ca conductance dependent on entry of Ca ions in molluscan

neurons. *Proc. Natl. Acad. Sci. USA.* 76:1497–1500.

Tsien, R. W. 1983. Calcium channels in excitable cell membranes. *Annu. Rev. Physiol.* 45:341–358.

Weidmann, S. 1955. Effects of calcium ions and local anaesthetics on electrical properties of Purkinje fibers. *J. Physiol. (Lond.).* 129:568–582.

Wilson, D. L., K. Morimoto, Y. Tsuda, and A. M. Brown. 1983. Interaction between calcium ions and surface charge as it relates to calcium currents. *J. Membr. Biol.* 72:117–130.